

Molecular Transport of a Magnetic Nanoparticle Swarm Towards Thrombolytic Therapy

Laliphat Manamanchaiyaporn^{ID}, Xiuzhen Tang, Yuanyi Zheng, and Xiaohui Yan

Abstract—Due to miniature size, controllability, navigation and versatile capability, micro/ nanorobots is appealing for minimally invasive procedures. In particular, blood clot as an unwanted biological object in vessel leads to severe diseases. Herein, we report a magnetite nanoparticle swarm (Fe_3O_4) that is capable of inducing hydrodynamic effect to capture tissue plasminogen activator (t-PA) in emergent vortices under the dynamic magnetic field. Once the swarm move to approach a site of a blood clot, the caged t-PA molecules are transported together with it across the interface for thrombolysis. In addition, the dynamic motion of each individual spinning nanorobot can assist the clot removal by exerting mechanical force to rub against the softened clot with loose fibrin fibers that is incompletely dissolved by chemical lysis of t-PA. Feasibility and performance of the swarm towards thrombolytic therapy are approved by *in vitro* experiments. The result reports that blood clot with 3-mm-diameter and 9-mm-length is completely removed in two hours, faster than the clinical procedure applying t-PA alone about 3 times. The contribution is extensible to apply for medical treatments ranged from simple tasks (e.g. detoxification) to complex tasks (e.g. tumor destroy).

Index Terms—Micro-/ nanorobotics, medical robots, magnetic micro-/ nano swarm.

I. INTRODUCTION

FOR YEARS, micro/ nanorobots have shown potential and become promising in wide-ranging medical applications towards minimally invasive intervention and therapy (e.g. ablation, biopsy) [1]–[3]. Magnetic field produced by actuation system (e.g. electromagnet, moving magnets) was one of sources implemented to power miniature magnetic robots and tools to fulfil biomedical applications [4]–[7]. Apart from the actuation system, smart and soft materials embedded with magnetic

particles were employed to fabricate small-scaled robots to carry out effective locomotion and controllable structures provided by magnetic compliance with a minimal control of magnetic field [8]–[10]. Star-like grippers with a soft structure were thermally triggered for grasping tissues towards *in vivo* biopsy devices after reaching the set-point temperature [11]. A hard-bodied helical millirobot utilized its helical propulsion to drill through *in vitro* blood clot under the driving of the rotating magnetic field generated by two synchronized permanent magnets [12]. A screw-head robot responded to rotating magnetic field for forward propulsion to drill through *in vitro* tissue [13]. Biohybrid helical microrobots with a hollow core promising a drug loading were deployed into mouse's insides for *in vivo* tumor therapy with ultrasound-image guidance [14]. A helical-shelled microrobot was magnetically controlled to carry immotile sperm cells to oval for assisting an *in vitro* fertilization [15].

Although an individual miniature robot could contribute great results to various applications, in order to treat inside human's parts and inaccessible or hard-to-reach regions, the functions and tiny size of robots is preferable, as well as a vast number of collaborative micro- and nanorobots with an independent drive and locomotion capabilities would be an alternative and feasible strategy to treat further applications. In a poisonous region, 3D-printed micro-fish were deployed to treat *in vitro* detoxification under magnetic guidance and chemical propulsion caused by additionally reactive nanoparticles [16]. Magneto-aerotactic behavior of bacteria navigated by magnetic field was used to deliver drug to the cancer cell for precisely targeted therapy [17]. A swarm of artificial bacterial flagella was navigated in the peritoneal cavity of a mouse for *in vivo* cancer therapy [18]. Due to and electrostatic interaction between dipoles, magnetite particles could attract each other to become a larger cluster. This phenomenon benefited further for a locomotion system and microfluidic applications. For example, duo to having long strip, artificial magnetic cilia were utilized as micromixers to induce microfluidic effect in mixing channel of medium, and resulted the higher-mixing efficiency and effectiveness even at $Re < 1$ [19]–[21]. Locomotion styles of particle swarm could reconfigure based on types of the dynamic magnetic field that was applied to form the swarm. The rotating field about the horizontal axis could roll long particle chains for moving on plane. The chains could be broken into fragments, and then reform the chain by the change of parameters of the actuating magnetic field (e.g. frequency) as well as hydrodynamic drag of media plays an important role for a swam generation and transformation [22]–[24].

However, functional capabilities of micro-/ nanoscale robots still remain challenges in medical interventions. In particular, behavior of a massive number of those controllable tiny particles as called a swarm would benefit to treat abnormal and unwanted

Manuscript received October 16, 2020; accepted February 15, 2021. Date of publication March 25, 2021; date of current version May 27, 2021. This letter was recommended for publication by Associate Editor L. Zhang and Editor X. Liu upon evaluation of the reviewers' comments. This work was supported by Thammasat University Research Fund (No. TUFT32/2564) and Faculty of Engineering, Thammasat University, Thailand. (Laliphat Manamanchaiyaporn and Xiuzhen Tang contributed equally to this work.) (Corresponding authors: Laliphat Manamanchaiyaporn; Yuanyi Zheng; Xiaohui Yan.)

Laliphat Manamanchaiyaporn is with the Department of Mechanical Engineering, Thammasat University, Pathum Thani 12120, Thailand (e-mail: mlalipha@engr.tu.ac.th).

Xiuzhen Tang and Yuanyi Zheng are with the Department of Ultrasound in Medicine and Shanghai Institute of Ultrasound in Medicine, Sixth People's Hospital Affiliated to Shanghai Jiao Tong University, Shanghai 200233, China (e-mail: tangxiuzhen8@163.com; zhengyuanyi@163.com).

Xiaohui Yan is with the Center for Molecular Imaging and Translational Medicine, School of Public Health, Xiamen University, Xiamen 361005, China (e-mail: xhyan@xmu.edu.cn).

This letter has supplementary downloadable material available at <http://ieeexplore.ieee.org>.

Digital Object Identifier 10.1109/LRA.2021.3068978

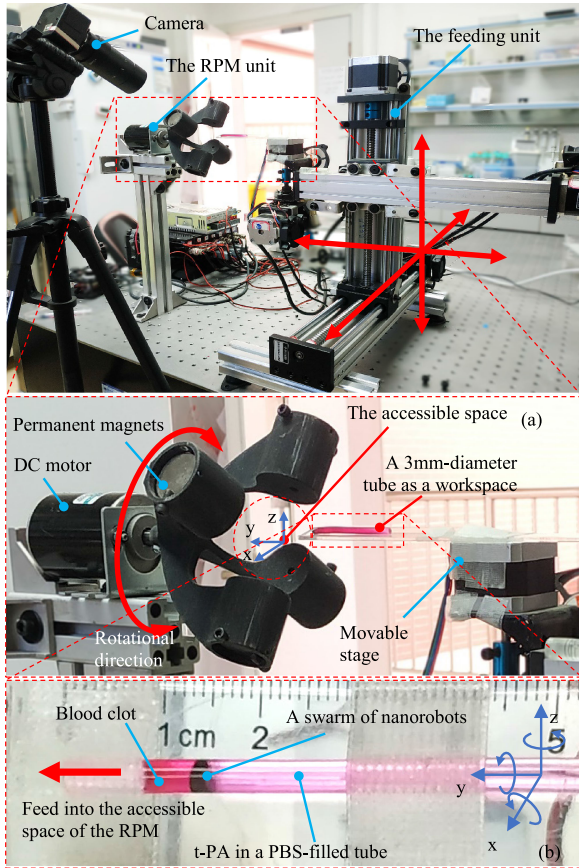


Fig. 1. Magnetic actuation system. (a) Two units consisting of the rotating permanent magnet unit (RPM, left) and the 6-DOF-feeding unit (right). (b) A scheme of a nanorobot swarm to remove *in vitro* clot within a tube as a movable workspace placed on the stage of the feeding unit.

objects. Blood clots as called thrombus are semisolid clumps that form and stationary in veins or arteries, which cause many severe diseases by blocking the flow of blood. One of challenges to treat thrombolysis was presented by using magnetic nanorods to enhance the acceleration of t-PA diffusion at the clot interface, another was about employing magnetic chain-cored soft microrobots inspired by magnetosome which delivered and released t-PA via magneto-collective control, and another was about deploying magnetic nanoparticle swarm to the clot site and then induced the convective flow to accelerate t-PA molecules [25]–[27]. All of them were promising for ultra-minimal invasive thrombolysis. On the other hands, in this work, we apply a swarm of nano-scaled robots (Fe_3O_4 nanoparticles) for *in vitro* thromolytic therapy. The swarm controlled by the new aspect of the dynamic magnetic field can induce the hydrodynamic effect to trap nearby molecules in the eye of an emergent vortex, then transport them together to the targeted site [28]. Under this concept, according to a scheme depicted in Fig. 2(a), in the presence of non-moving nanorobots and tissue plasminogen activator (t-PA) in vessel with a blood clot, with no magnetic actuation, t-PA as thromolytic agents typically diffuses across the boundary over a time, and then approaches and dissolves the clot gradually. The higher concentration of t-PA, the faster the diffusive rate. On the other hand, exhibited in Fig. 2(b), once the rotating magnetic field is operated to spin each individual nanorobot, those magnetic nanorobots form a swarm to

transport the caged t-PA molecules to dissolve the clot effectively and precisely, based on chemical lysis of t-PA and mechanical rubbing of the swarm.

The work provides new insights into behavior of a swarm as an active system where the collective motion to treat blood clot is caused by an interplay of the nanorobotic swarm and nearby t-PA molecules under the driving of the translating-rotating magnetic field. The letter is organized as the following: section II provides a protocol of magnetic actuation to manipulate a swarm of nanorobots, which consists of the designed actuation system, modeling of magnetic actuation. Section III presents experimental validations by applying the dynamic motion of the swarming nanorobots. Next, section IV provides conclusion. Finally, Appendix contains experimental details and preparations.

II. MAGNETICALLY ACTUATING PROTOCOL TO MANIPULATE A SWARM OF NANOROBOTS

A. Magnetic Actuation System

Magnetic actuation system is specifically designed on the basis of magnetic manipulation using a 6-DOF movable workspace within the 1-DOF rotating magnetic field. It consists of two co-operating units, depicted in Fig. 1. The first, a stationary unit of rotating permanent magnets (RPM) contains four permanent magnets (two perpendicular couples of two coaxially arranged magnets, 30-mm-diameter and 30-mm-long, cylindrical, axially magnetized N52-graded NdFeB, the maximum strength on surface about 350 mT). The magnets are all arranged in a 3D-printed case that is built-in with a suspension to reduce vibration and mount on a 24 VDC motor (Manasin Inc.) which is set up on a stationary platform. The rotational speed of the motor is adjustable between 0–50 Hz without vibration. The case provides an accessible space about $60 \text{ mm} \times 60 \text{ mm} \times 70 \text{ mm}$, depicted in Fig. 3(a). Superimposed magnetic field strength is about 30 mT at the center of the four-magnet arrangement, measured by a gaussmeter (GM-08 Hirst). Next, the second, a feeding unit is a 6 DOF-movable stage (three-translation and three-rotation along the principal axis by 6 servomotors), and it functions to move a workspace set up above. Thus, in the case that the workspace contains nanorobots, its moving into or out of the accessible space of the RPM is able to passively change the position of the swarm in the workspace.

Magnetic field produced by a permanent magnet basically contains a strong magnetic force exerted by magnetic gradient. However, a main purpose to employ the coaxial arrangement of those couple magnets is about no deviation and drifting of the controlled robots due to no force interference in the homogeneous region. The arrangement minimizes magnetic force, especially in a homogeneous region of magnetic field, where is overwhelmed by magnetic torque. In order to indicate the homogeneous region (homogeneity < 1%), COMSOL Multiphysics is applied to investigate the superposition of magnetic field produced by the four-magnet arrangement, depicted in Fig. 3(a). The results report the homogeneous region of rotating magnetic field about $\varnothing 8 \times 10 \text{ mm}^3$, exhibited in Fig. 3(b) and (c). Next, in Fig. 3(d), the behaviors of the swarm nanorobots are different, when they are induced at the different position in the field, depicted. At the position I where is the center of the RPM, the nanorobots are fully distributed across the boundary, caused by homogeneous magnetic field which exerts only magnetic torque. On the other hand, at the position II, III, IV and V where

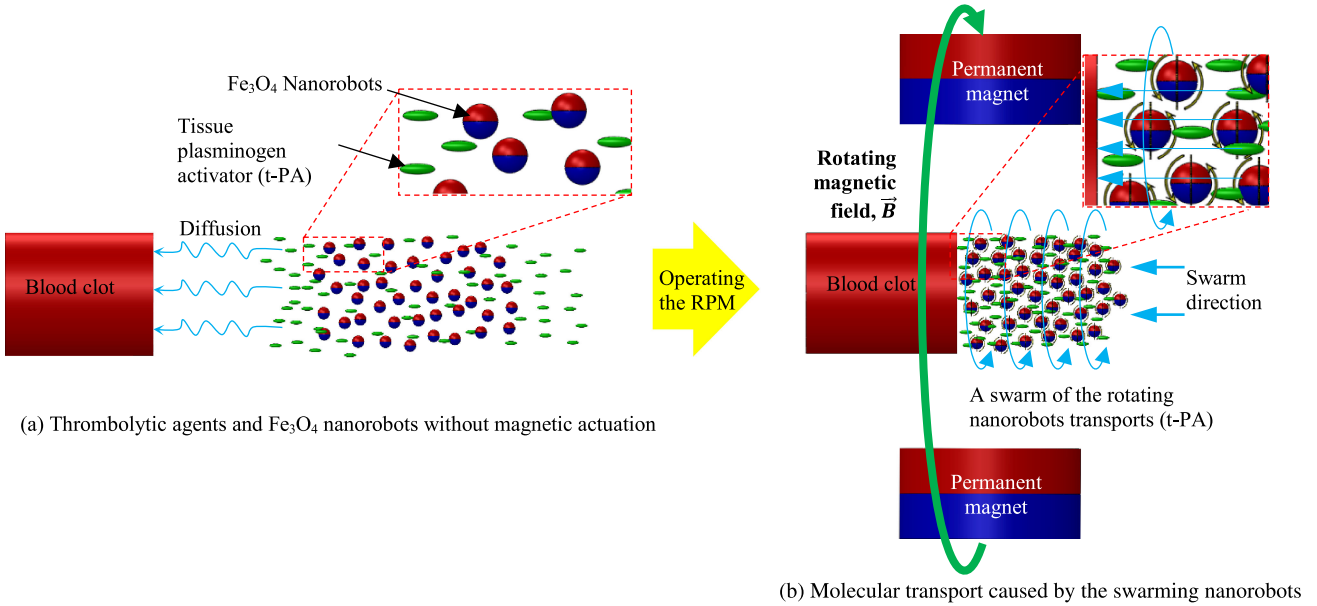


Fig. 2. A scheme of the actuation protocol for blood clot removal by a swarm of nanorobots and tissue plasminogen activator (t-PA). (a) No magnetic actuation, t-PA normally diffuses in media. (b) When the RPM is operated, the rotating magnetic field actuate nanorobots to become a swarm to trap and transport thrombolytic molecules to the clot site.

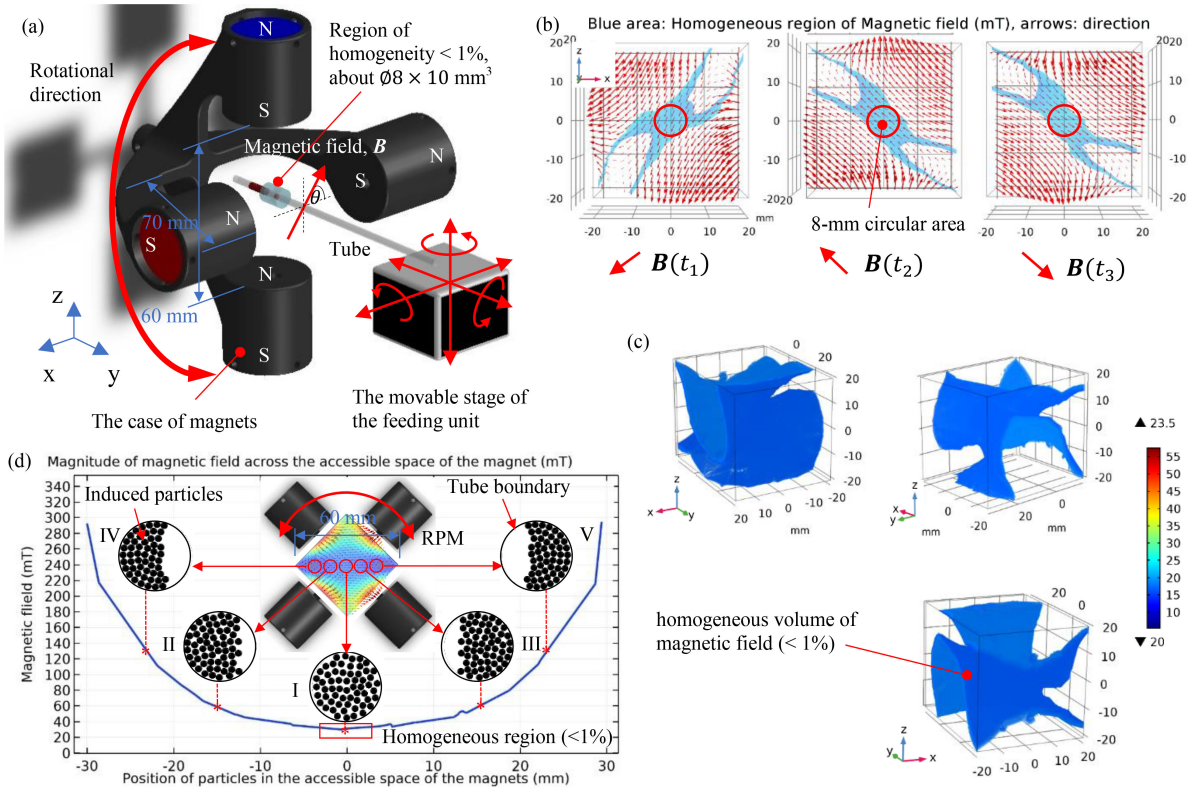


Fig. 3. The rotating permanent magnets (RPM) and magnetic field characteristics. (a) The RPM consists of two coupling magnets (N and S represent North and South pole), and provides 60 mm × 60 mm × 70 mm of an accessible space and Ø8×10 mm³ region of a homogeneous magnetic field (<1%). A tube as a workspace is set up on a movable stage in order to passively changes the position of the nanorobot swarm. (b) In the radial plane of the tube, the blue area depicts the superposition of the homogeneous magnetic field (<1%) produced by four permanent magnets, and (c) 3D-graphical images show the homogeneity (1%) of magnetic field. Once the RPM rotates, an overlap area of the rotating field is identified about Ø8×10 mm³. (d) The plot of magnetic field strength against the position along the horizontal axis of the accessible space shows the uniform curve which reports the homogeneous region at the center of the RPM. Each of the position significantly affects how the swarm distributes across the tube. Once it is in the region, resulting in the uniform distribution, but when it is out of the region, the existence of magnetic force will pull it to lean on the side of the tube.

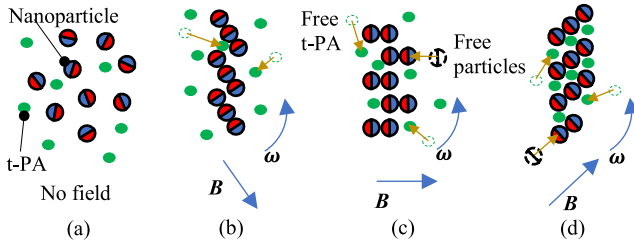


Fig. 4. A possible scheme of a t-PA capturing procedure of a nanoparticle swarm formed by the rotating magnetic field. (a) t-PA and nanoparticles are dispersed in media with no actuating magnetic field. (b) once the field is on, each individual particle aligns with the direction of the field and attracts each other to start forming nanochains. (c), (d) meanwhile the field is rotating, long particle chains are disassembled into small clusters, then those separated pieces are reversibly into the long chains again, and then simultaneously induces hydrodynamic effect to capture t-PA in the emergent vortices of the rotating chains. Based on this concept, free particles and small clusters are attracted to be a member in the other formed chains which makes the swarm larger to cage more t-PA inside.

locate outside the homogeneous region of magnetic field, the induced robots lean on either side of the boundary, due to the influence of the pulling magnetic force.

A dynamic magnetic field is capable of forming the spreading nanoparticles into long chains, and reversibly disassemble the chains into smaller clusters [24], and the characteristics and contributions of forming or breaking chains that concern the applied magnetic field, fluidic environment and substrate condition are applied further. Therefore, depicted in Fig. 4, once the nanoparticles are operated in the homogeneous region of the rotating magnetic field, the reversibility between assembly and disassembly process of the rotating nanoparticle chains are capable to induce hydrodynamic effect, and then emerge vortices to trap t-PA molecules inside [28]. In addition, angular speed of the swarm is proportional to the frequency of rotating magnetic field which synchronizes to rotational speed of the motor. It directly affects the performance of the emergent vortices to trap nearby molecules. However, due to non-movability of the RPM, the vortices are held at the central position of the couple magnets. The workspace placed on the feeding unit is instead moved in order to passively mobilize the swarm. That is, the change in the position of the swarm is passive by the active movement of the workspace. Thus, the molecules which are trapped in the vortices, locomotion of the swarm causes the transport of the caged molecules to the targeted location. Besides, if molecules are diffusive, instead of normal diffusion, the protocol to swarm and transport can accelerate the diffusivity of the molecules significantly.

B. Modeling of Magnetic Actuation

Magnetic response of a nanorobot depends on the rotating permanent magnets (RPM) placed over the robot. Magnetic field and gradient produced by the RPM are mapped based on the analysis presented in [29]. Thus, in Fig. 5, considering the dipole model based on a spherical coordinate system, scalar potential of the RPM is approximated at a nanorobot position (\mathbf{r}) as the following,

$$\Phi_M = (\mathbf{r}, \theta, \mathcal{Z}) = \frac{1}{4\pi} \int_V \frac{\nabla \cdot \mathbf{M}}{|\mathbf{r} - \mathbf{p}|} dV_M \quad (1)$$

where \mathbf{M} is the magnetization vector of the permanent magnet, \mathbf{p} is a position vector to be integrated over the volume of the

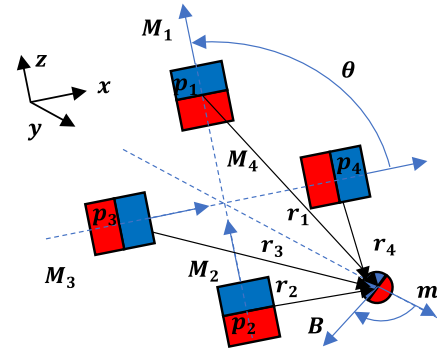


Fig. 5. Dipole model of the magnetic interaction between the RPM and a magnetic nanorobot.

permanent magnet, and dV_M is the infinitesimal segment in the volume. The gradient of Φ_M provides the magnetic field, which is

$$\mathbf{B} = -\mu_0 \nabla \Phi_M \quad (2)$$

where μ_0 is the permeability of free space. Once the magnetic field (\mathbf{B}) is calculated for the four permanent magnets, the magnetic force (\mathbf{F}_m) and magnetic torque (\mathbf{T}_m) exerted on the nanorobot are calculated by

$$\begin{bmatrix} \mathbf{F}_m \\ \mathbf{T}_m \end{bmatrix} = \begin{bmatrix} \mathbf{m} \cdot \nabla (\mathbf{R}_1 \mathbf{B}_1 + \dots + \mathbf{R}_4 \mathbf{B}_4) \\ \mathbf{m} \times (\mathbf{R}_1 \mathbf{B}_1 + \dots + \mathbf{R}_4 \mathbf{B}_4) \end{bmatrix} \quad (3)$$

where $\mathbf{R}_1, \dots, \mathbf{R}_4$ are the rotation matrices from frames of four permanent magnets to the frame of the nanorobot, and $\mathbf{B}_1, \dots, \mathbf{B}_4$ are the magnetic fields of the four permanent magnets. \mathbf{m} is the total magnetization of particle chains formed by magnetic interaction force between dipole moment of each individual particle, which is expressed by

$$\mathbf{m} = V_c \chi \frac{\mathbf{B}}{\mu_0} \quad (4)$$

where V_c is volume of the chain, and χ is the magnetic susceptibility constant of the nanoparticles.

As mentioned, it is due to the fact that the swarm is controlled by the rotating homogeneous magnetic field. This enables us to only apply a pure magnetic torque on the robot, but in order to change the position of the swarm in the workspace, the movable workspace is fed into the boundary of the homogeneous region instead. Any deviation in the position of the robot only exists along the y-axis that contributes to the propulsion force of the swarming nanorobots, caused by the translation of the workspace.

Reynolds number of the swarm is calculated by $Re = \frac{\rho v l}{\mu}$, where ρ is the density of the fluid (1060 kg.m^{-3}), v is velocity of the nanorobot and l is its diameter ($300 \times 10^{-9} \text{ m}$), and μ is the dynamic viscosity of the fluid ($1.05 \times 10^{-3} \text{ Pa.s}$). Due to the size in nanoscale, the calculated Reynolds number is definitely low than 1 ($Re < 1$). Then, the swarm can be modeled based on a torque, force and a Stokes' induced creeping flow at low Reynolds number. Therefore, the motion of the rotating robots is governed by

$$\begin{bmatrix} \mathbf{F}_m + \mathbf{F}_g + \mathbf{F}_d + \mathbf{F}_c + \mathbf{F}_f \\ \mathbf{T}_m + \mathbf{T}_g + \mathbf{T}_d + \mathbf{T}_c + \mathbf{T}_f \end{bmatrix} = Z \begin{bmatrix} \mathbf{v} \\ \omega \end{bmatrix} \quad (5)$$

where \mathbf{F}_d and \mathbf{T}_d denote the viscous drag force and torque, respectively. \mathbf{F}_f and \mathbf{T}_f are the interactive or fretting force and

torque between the nanorobots and the clot, respectively. \mathbf{F}_c and \mathbf{T}_c denote the reaction force and torque when the robot is in contact with the tube surface. \mathbf{F}_g and \mathbf{T}_g are the force and torque exerted on the robot due to gravity. Next, \mathbf{v} and ω are linear velocity and angular velocity, respectively. \mathbf{Z} is the overall hydrodynamic resistance matrix [12].

Diffusion is the gradual movement or dispersion of molecules within a boundary, due to a concentration gradient. In the case of t-PA injection to dissolve blood clot in media, the t-PA molecules diffuse gradually over the interface. According to the Von Smoluchowski's equation [26], [30], the rate for a diffusion-limited reaction is given by

$$k_T = 4\pi D_{t-PA} (R_{t-PA} + R_{site}) C_{t-PA} \quad (6)$$

where D_{t-PA} is the effective diffusivity of t-PA, R_{t-PA} and C_{t-PA} are the radius and concentration of t-PA molecules, R_{site} is radius of lysine sites.

According to the scheme of Fig. 2, the swarm of nanorobots is capable of enhance the hydrodynamic effect. The diffusivity is remapped as the following,

$$D_{t-PA} = D_{t-PA}^T \left(1 + \frac{2}{3\pi^2} Pe^2 \right) \quad (7)$$

where D_{t-PA}^T is the thermally induced diffusion coefficient given by Stokes-Einstein's equation, which is

$$D_{t-PA}^T = \frac{k_B T}{6\pi n R_{t-PA}} \quad (8)$$

where k_B , T and n are the Boltzmann constant, temperature, and viscosity of t-PA solution, respectively, and the Peclet number, Pe is defined by

$$Pe = \frac{\mathbf{v} C_{NR}^{-1/3}}{D_{t-PA}^T} \quad (9)$$

where C_{NR} is concentration of the nanorobots and \mathbf{v} is the average velocity of the flow field induced by the swarm. From eq. (6), (7) and (9), it can be analyzed that the rate of clot removal depends on the diffusivity of t-PA which can be enhanced by the Peclet number in the term of velocity of the swarm. Based on t-PA molecules transported by the swarm, the faster the velocity of the swarm, the higher the acceleration rate of molecular diffusion, the higher the rate of clot removal.

III. MOLECULAR TRANSPORT BY A SWARM OF MAGNETITE NANOROBOTS

A. A Swarm of Nanorobots Driven by the Rotating Magnetic Field in the Homogeneous Region

A tube with $\varnothing 3$ -mm-diameter and 10-cm-long contains the suspension of Fe_3O_4 nanoparticles ($400 \mu\text{g}/\text{mL}$) in phosphate buffered saline (PBS solution). It is set up on the stage of the feeding unit, depicted in Fig. 6. Once the RPM is operated to produce the rotating magnetic field, nanoparticles in the tube are rotationally driven to swarm and induce vortices in the media. Obviously, the swarm properly distribute across the cross-sectional area of the tube because the tube locates in the homogeneous region of magnetic field. Moreover, its angular velocity directly synchronizes to the rotational speed of the RPM. The faster the rotational speed, the higher rate the hydrodynamic effect to capture molecules in the emergent vortices. The propulsion of the swarm is a passive action caused by the movable tube set up on the feeding unit. Thus, its translation

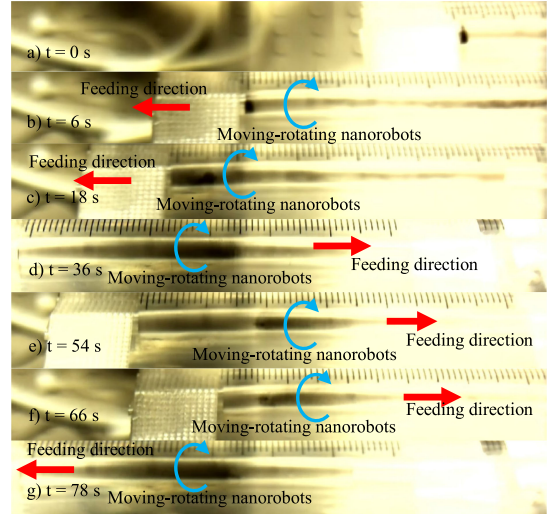


Fig. 6. Magnetic suspension (Fe_3O_4) in a PBS filled tube under the rotating magnetic field. (a) to (g) a time-lapse sequence of the nanoparticle swarm actuated by the field. The swarm can passively change the position by moving the tube into/ out the homogeneous field via the feeding unit.

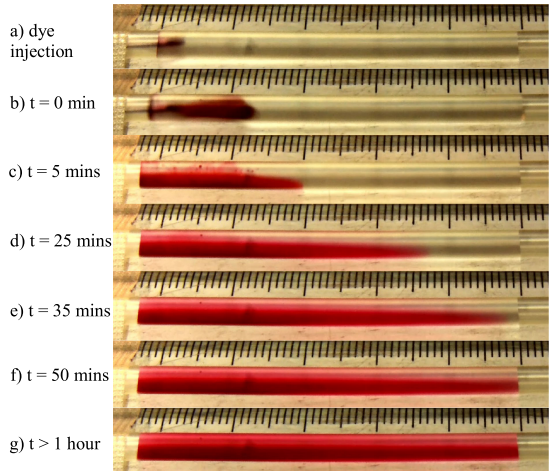


Fig. 7. Normal diffusion of the dye solution in the PBS solution filled in a tube. (a) to (g) a time-lapse sequence of the dye molecules diffusely creeping over the tube. Time usage more than an hour to complete the entire process.

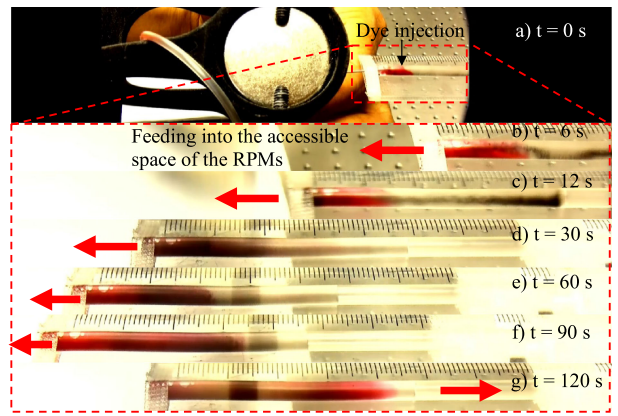


Fig. 8. Dye-molecular transport by the swarm of nanorobots. (a) to (g) a time-lapse sequence of the dye molecules being trapped and transported promptly and quickly to any location where the swarm passes.

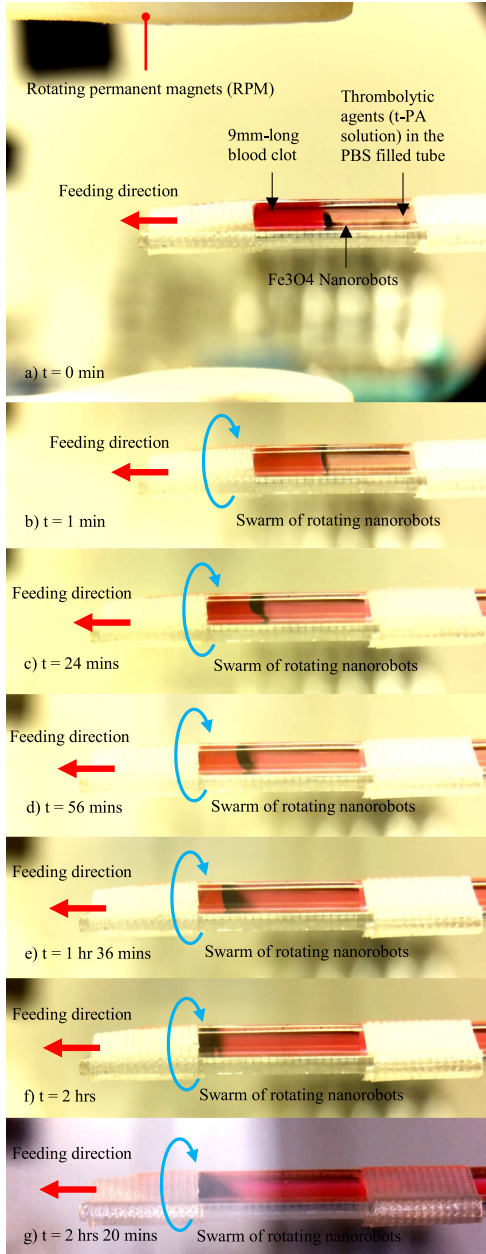


Fig. 9. A swarm of rotating magnetic nanorobots transporting thrombolytic agent to remove the blood clot. (a) to (g) a time-lapse sequence of the clot removal.

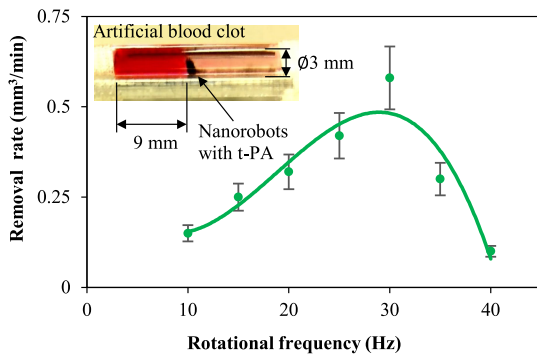


Fig. 10. The plot of the rate of clot removal against the different rotational frequency of the RPM. (clot volume: 63.59 mm^3).

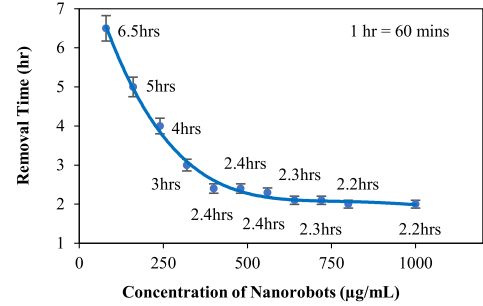


Fig. 11. The plot of clot removal time against the different concentration (ranged from 80 to 1000 $\mu\text{g}/\text{mL}$) of nanorobots, (unit: hour).

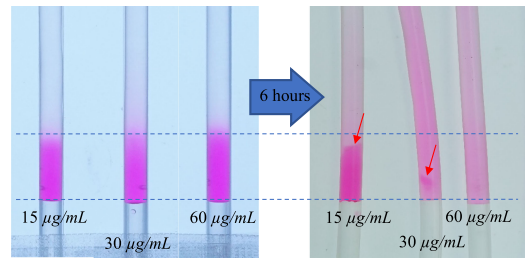


Fig. 12. Normal chemical lysis by injecting three concentration of t-PA (15, 30 and 60 $\mu\text{g}/\text{mL}$) into the clot fabricated in the tube.

promptly responds to the change in a position of the tube. (Supplementary video 01)

B. Normal Diffusion of Dye Molecules VS Molecular Transport (Diffusion Accelerated) by a Swarm of Nanorobots

In Fig. 7, dye solution ($20 \mu\text{L}$) is injected into a tube filled with 5 cm-long PBS solution, and then let it diffuse normally across the tube by time. Obviously, the diffusive rate of the injected dye is low. It creeps from the injection point to the opposite point of the tube. Finally, more than an hour, the dye diffuses completely. (Supplementary video 02)

On the other hand, as mentioned, the swarm is capable of inducing the hydrodynamic effect to pull nearby molecules into the region of the swarm, then capture them in the emergent vortices, and then transport them together with its propulsion. Depicted in Fig. 8(a), a tube filled with PBS solution is set up on the stage of the feeding unit, then dye solution ($20 \mu\text{L}$) is injected at a side of the tube, and then the magnetic suspension (Fe_3O_4 nanoparticles: $400 \mu\text{g}/\text{mL}$) is injected at the opposite side. Next, once the RPM is operated to generate the rotating magnetic field, and simultaneously the tube is fed into the region of the field, nanoparticles start forming a swarm, exhibited in Fig. 8(b), (c). The motion of swarm traps the dye molecules in the induced vortices, depicted in Fig. 8(d). When the tube is continuously fed into the region of magnetic field to passively change the position of the swarm, the dye molecules caught in the swarm is promptly moved to any location where the swarm passes as fast as is its translation speed. The change of the transparent color of the PBS to the pink color of the dye color is an obvious result to approve that the dye molecules is transported by the swarm, shown in Fig. 8(e)–(g). In another word, diffusivity of the dye is accelerated by the swarm significantly. This protocol

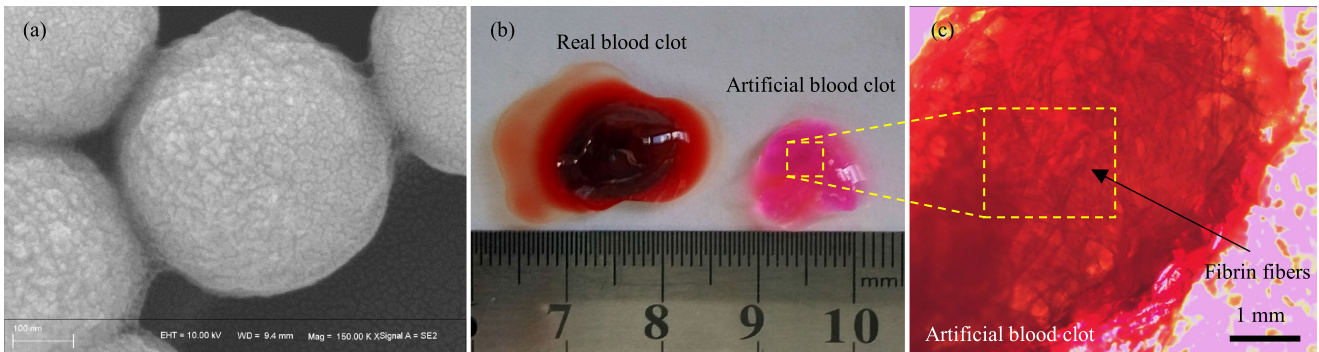


Fig. 13. Supplementary images. (a) A SEM image of magnetic nanoparticles; sphere, avg. 500 nm. (b) Comparison between the real blood clot and artificial blood clot. The artificial blood clot seems transparent, because there is no Hemoglobin as a red protein to color clot with red. It is solely responsible for the transportation of oxygen in the blood, and does not affect blood clotting. (c) Microscopic image of artificial blood clot.

shortens the time of normal diffusion extremely. (Supplementary video 03)

C. In Vitro Blood Clot Removal by Tissue Plasminogen Activator (t-PA) Transported by a Swarm of Nanorobots

A magnetic nanoparticle swarm does not only accelerate the diffusivity of molecules with the time extremely shorter than the normal diffusion, but its rotating motion also advantages to exert the mechanical force to rub against nearby matters interestingly, especially to remove a blood clot in vessel. Clinically, thrombolytic drug may apply to dissolve the clot via an injection into the vessel and let it flow with blood to the clot site. However, the effect of the drug needs time consuming, and it may not work properly, precisely and effectively, including the beware of the side effect from overdose. Therefore, *in vitro* experiment is conducted in order to confirm the feasibility and performance of the nanorobotic swarm as a medical device for thrombolytic therapy.

In Fig. 9, a 9 mm-long *in vitro* artificial blood clot is fabricated in a 3 mm-diameter silicone tube (see fabrication process in Appendix). Next, the tube is filled with PBS solution, then nanorobots (Fe_3O_4 magnetic suspension: 400 $\mu\text{g}/\text{mL}$), and then tissue plasminogen activator (t-PA: 30 $\mu\text{g}/\text{mL}$). Concentration of t-PA is chosen at a dose based on unharmed amount for clinical use about 16–30 $\mu\text{g}/\text{mL}$ (see Appendix). When the RPM is operated at 30 Hz to generate the rotating magnetic field, and then the tube is fed into the field, the swarm is formed, simultaneously induces the hydrodynamic effect to pull and cage t-PA molecules into the emergent vortices, and conveys them to the clot site. After reaching the clot, chemical lysis of t-PA dissolves the solid clot to become colored fluid and the softened clot with loose networks (fibrin fibers). Besides, the dynamic motion of the swarm exerts mechanical force to assist in rubbing against the clot alternatively. The dissolved clot is obviously noticed by the change in the original color of PBS solution into the color of the clot, from the transparent to pink color. The entire process to remove the clot completely takes around 2 hours and 20 minutes. (Supplementary video 04)

In addition, in Fig. 10, rotation frequency of the RPM significantly increases the removal rate which is maximum about 0.53 mm^3/min at 30 Hz, but sharply drops after reaching the step-out frequency ($>30\text{Hz}$). In Fig. 11, different concentrations of magnetic suspension (80, 160, 240, 320, 400, 480, 560, 640, 720, 800, 1000 $\mu\text{g}/\text{mL}$) are investigated about the time to complete the clot removal. The results show that the increasing

number of concentrations significantly exponentially reduces the time to remove the clot. The 80, 160, 240 and 320 $\mu\text{g}/\text{mL}$ takes about 6, 5, 4 and 3 hours to complete the action, respectively. In contrast, when the concentration is gained from 400, 480, 560, 640, 720, 800 and 1000 $\mu\text{g}/\text{mL}$, the removal time slightly decreases from 2.4, 2.4, 2.4, 2.3, 2.3, 2.2 and 2.2 hours respectively, and it tends to be stable even though the concentration is gained more than 1000 $\mu\text{g}/\text{mL}$. The reason concerns the crowd of nanoparticles that possibly blocks each other from approaching the clot as well as it may obstruct t-PA to pass through the clot. The removal rate in experiments are corresponding to the rate mapped in theoretical models which mainly concern the induced flow velocity, concentration and rubbing of the swarm.

In order to compare with the clot removal by a swarm, clinical treatment of thrombolysis by only t-PA agents is experimented to observe the removal time. According to the plot in Fig. 12, three concentrations of t-PA which are 15, 30 and 60 $\mu\text{g}/\text{mL}$ is injected into the clot in three tubes. The results report that only 60 $\mu\text{g}/\text{mL}$ completely removes the clot in 6 hours, but 15 and 30 $\mu\text{g}/\text{mL}$ still remain the clot about 30% and 5% respectively, which mostly sticks on the surface of the tube. Therefore, an intervention of the swarm as a controllable thrombolytic agent can improve blood clot-cleaning efficiency and still reduce the treatment time almost 3 times when comparing to the clinical method for thrombolytic therapy.

IV. CONCLUSION

A new concept of the magnetic manipulation is exposed to carry out thrombolytic therapy performed by a swarm of Fe_3O_4 nanoparticles that is magnetically manipulated to capture t-PA molecules in the emergent vortices, and then convey them together with its locomotion to a blood clot site. Firstly, the comparison of the normal diffusion and the magnetic swarm-assisted diffusion of the dye molecules is experimented to distinguish the better performance and faster time of the molecular-transportation. Finally, the swarm driven by the rotating magnetic field is employed to transport thrombolytic agents (t-PA) for the *in vitro* blood clot removal, caused by chemical dissolution of t-PA and mechanical rubbing of the swarm. In addition, the swarm can completely remove the clot in 2 hours. The removing time may be long because the size of the clot is bigger than the real clot in vessel about 2 times. Thus, if the size of the clot is smaller. The time to remove it would be

significantly shorter. This contribution is extensible to treat other minimally invasive interventions ranged from detoxification to tumor treatment.

APPENDIX

Supplementary note: Experimental details and preparations

The RPM is operated at the 30 Hz as the best parameter for all experiments according to the plot in Fig. 10.

The size of the transparent silicone tube is 3 mm-diameter.

Fe_3O_4 magnetic nanoparticles was purchased from Sigma-Aldrich (500 nm diameter, sphere, magnetization > 45 emu/g at 4500 oe), depicted by a SEM image in Fig. 13.

PBS (phosphate buffered saline) solution was purchased from Sigma-Aldrich. (density 1060 kg.m^{-3}), viscosity $1.05 \times 10^{-3} \text{ Pa.s}$)

Artificial blood clot preparation: 80 μL human thrombin (purchased from Sigma-Aldrich) was added to 1 mL of HPPP (human platelet poor plasma; purchased from Sigma-Aldrich), them was dyed with the light-pink color, and then all of them was well mixed by vortex. Next, the mixture was injected at an end of the Ø 3 mm-tube to form a 9 mm-long clot. Next, the tube was stored at 37 °C for 40 min. The fabricated clot was strongly bonded in the tube without loose. In Fig. 13, the artificial clot is compared to the real clot that is naturally formed from real blood. A microscopic image depicts fibrin of the artificial blood clot, exhibited in Fig. 13. The artificial blood clot seems transparent, because there is no Hemoglobin as a red protein to color clot with red. It is solely responsible for the transportation of oxygen in the blood, and does not affect blood clotting.

Thrombolytic agents (tissue plasminogen activator: t-PA, Activase, Genetech Inc., USA): t-PA solution with 30 $\mu\text{g/mL}$ concentration was liquefied from its lyophilized powder. In order to calculate unharful concentration of t-PA, total dose to use t-PA for Occlusion (Ischemic stroke) does not exceed 100 mg for patient's weight $\geq 67 \text{ kg}$ [31], so the maximum safety dose is rewritten to 1.5 mg/kg. Human's blood volume is about 50 to 90 mL/kg, so concentration per a dosage is about 16 to 30 $\mu\text{g/mL}$

ACKNOWLEDGMENT

The authors would like to thank Xiamen University for laboratory. The first author sincerely thanks Prof. Xiaohui Yan, as a teacher, for opportunity and advice on research.

REFERENCES

- [1] J. Wang and W. Gao, "Nano/Microscale motors: Biomedical opportunities and challenges," *ACS Nano*, vol. 6, no. 7, pp. 5745–5751, 2012.
- [2] B.J. Nelson, I.K. Kaliakatsos, and J.J. Abbott, "Microrobots for minimally invasive medicine," *Annu. Rev. Biomed. Eng.*, vol. 12, pp. 55–85, 2010.
- [3] J. Liu, J. Wen, Z. Zhang, H. Liu, and Y. Sun, "Voyage inside the cell: Microsystems and nanoengineering for intracellular measurement and manipulation," *Microsyst. Nanoeng.*, vol. 1, 2015, Art. no. 15020.
- [4] L. Manamanchaiyaporn, T. Xu, and X. Wu, "An optimal design of an electromagnetic actuation system towards a large homogeneous magnetic field and accessible workspace for magnetic manipulation," *Energies*, vol. 13, no. 4, pp. 911–934, 2020.
- [5] D. Son, H. Gilbert, and M. Sitti, "Magnetically actuated soft capsule endoscope for fine-needle biopsy," *Soft Robot.*, vol. 7, no. 1, pp. 10–21, 2020.
- [6] S. Jeon *et al.*, "A magnetically controlled soft microrobot steering a guidewire in a three-dimensional phantom vascular network," *Soft Robot.*, vol. 6, no. 1, pp. 54–68, 2019.
- [7] L. Manamanchaiyaporn, T. T. Xu, and X.Y. Wu, "The hybrid system with a large workspace towards magnetic micromanipulation within the human head," in *Proc. IEEE/RSJ Int'l. Conf. on Intel. Robot. Sys.*, 2017, pp. 402–407.
- [8] L. Manamanchaiyaporn, T. Xu, X. Wu, and H. Qian, "Roles of magnetic strength in magneto-elastomer towards swimming mechanism and performance of miniature robots," *Int. J. Robot. Autom.*, vol. 35, pp. 1–9, 2020.
- [9] L. Manamanchaiyaporn, T. Xu, and X. Wu, "Magnetic soft robot with the triangular head-tail morphology inspired by lateral undulation," *IEEE/ASME Trans. Mech.*, vol. 25, no. 6, pp. 2688–2699, Dec. 2020.
- [10] S. Palagi and P. Fischer, "Bioinspired microrobots," *Nat. Rev. Mat.*, vol. 3, pp. 113–124, 2018.
- [11] E. Gultepe *et al.*, "Biopsy with thermally-responsive untethered micro-tools," *Adv. Mat.*, vol. 25, pp. 514–519, 2013.
- [12] I. S. M. Khalil, A. F. Tabak, K. Sadek, D. Mahdy, N. Hamdi, and M. Sitti, "Rubbing against blood clots using helical robots: Modeling and in vitro experimental validation," *IEEE Robot. Autom. Let.*, vol. 2, no. 2, pp. 927–934, Apr. 2017.
- [13] A. W. Mahoney, N. D. Nelson, E. M. Parsons, and J. J. Abbott, "Non-ideal behaviors of magnetically driven screws in soft tissue," in *Proc. IEEE/RSJ Int'l. Conf. on Intel. Robot. Sys.*, 2012, pp. 3559–3564.
- [14] X. Yan *et al.*, "Multifunctional biohybrid magnetite microrobots for imaging-guided therapy," *Sci. Robot.*, vol. 2, 2017, Art. no. eaad1155.
- [15] M. Medina-Sánchez *et al.*, "Cellular cargo delivery: toward assisted fertilization by sperm-carrying micromotors," *Nano Lett.*, vol. 16, no. 1, pp. 555–561, 2016.
- [16] W. Zhu *et al.*, "3D-printed artificial microfish," *Adv. Mater.*, vol. 27, pp. 4411–4417, 2015.
- [17] O. Felfoul *et al.*, "Magneto-aerotactic bacteria deliver drug-containing nanoliposomes in tumour hypoxic regions," *Nat. Nano.*, vol. 11, pp. 941–947, 2016.
- [18] A. Servant, F. Qiu, M. Mazza, K. Kostarelos, and B. J. Nelson, "Controlled in vivo swimming of a swarm of bacteria-like microrobotic flagella," *Adv. Mat.*, vol. 27, no. 19, pp. 2981–2988, 2015.
- [19] S. Hanasoge, P. J. Hesketh, and A. Alexeev, "Microfluidic pumping using artificial magnetic cilia," *Microsyst Nanoeng.*, vol. 4, 2018, Art. no. 11.
- [20] E. S. Shanko, Y. van de Burgt, P. D. Anderson, and J. M. J. den Toonder, "Microfluidic magnetic mixing at low reynolds numbers and in stagnant fluids," *Micromachines*, vol. 10, p. 731–753, 2019.
- [21] I. Petousis, E. Homburg, R. Derkx, and A. Dietzel, "Transient behaviour of magnetic micro-bead chains rotating in a fluid by external fields," *Lab Chip*, vol. 7, pp. 1746–1751, 2007.
- [22] H. Xie *et al.*, "Reconfigurable magnetic microrobot swarm: Multimode transformation, locomotion, and manipulation," *Sci. Robot.*, vol. 4, no. 28, 2019, Art. no. eaav8006.
- [23] J. Yu and L. Zhang, "Reversible swelling and shrinking of paramagnetic nanoparticle swarms in biofluids with high ionic strength," *IEEE/ASME Trans. Mech.*, vol. 24, no. 1, pp. 154–163, Feb. 2019.
- [24] J. Yu, B. Wang, X. Du, Q. Wang, and L. Zhang, "Ultra-extensible ribbon-like magnetic microswarm," *Nat. Commun.*, vol. 9, no. 1, pp. 1–9, 2018.
- [25] M. Xie *et al.*, "Bioinspired soft microrobots with precise magnetocollective control for microvascular thrombolysis," *Adv. Mat.*, vol. 32, 2020, Art. no. 2000366.
- [26] R. Cheng *et al.*, "Acceleration of tissue plasminogen activator-mediated thrombolysis by magnetically powered nanomotors," *ACS Nano*, vol. 8, pp. 7746–7754, 2014.
- [27] Q. Wang, B. Wang, J. Yu, K. Schweizer, B. J. Nelson, and Li Zhang, "Reconfigurable magnetic microswarm for thrombolysis under ultrasound imaging," in *Proc. IEEE Int. Conf. Robot. Autom.*, pp. 10285–10291, 2020.
- [28] G. Kokot and A. Snezhko, "Manipulation of emergent vortices in swarms of magnetic rollers," *Nat Commun*, vol. 9, pp. 1–7, 2018, Art. no. 2344.
- [29] A. Mahoney and J.J. Abbott, "Five-degree-of-freedom manipulation of an untethered magnetic device in fluid using a single permanent magnet with application in stomach capsule endoscopy," *Int. J. Rob. Res.*, vol. 35, pp. 129–147, 2015.
- [30] D.F. Calef and J. M. Deutch, "Diffusion-controlled reactions," *Annu. Rev. Phys. Chem.*, vol. 34, pp. 493–524, 1983.
- [31] Activase: Important Safety Information & Indication, [Revised] Feb. 2018, Accessed on: Jan. 01, 2020, [Online], Available: <https://www.activase.com/safety.html>